DOI: 10.1002/anie.201200899

Drug-Delivery Systems

Self-Assembly of Thermally Responsive Nanoparticles of a Genetically Encoded Peptide Polymer by Drug Conjugation**

*Jonathan R. McDaniel, Jayanta Bhattacharyya, Kevin B. Vargo, Wafa Hassouneh, Daniel A. Hammer, and Ashutosh Chilkoti**

Most small-molecule therapeutic agents utilized in the clinic have poor bioavailability and suboptimal pharmacokinetics because of their hydrophobicity and low molecular weight. Engineered drug-delivery vehicles seek to improve the efficacy of these therapeutic agents by increasing their solubility, extending their plasma half-life, increasing the amount of drug deposited in the desired tissue, and decreasing their exposure to healthy tissues.[1] The repackaging of hydrophobic drugs by sequestering them within the core of soluble polymeric nanoparticles can overcome these limitations by increasing drug solubility; the appropriate choice of polymer can also lead to long in vivo circulation and improved tissue distribution as compared to that of the free drug.[1–4] Furthermore, the choice of stimulus-responsive polymers as the carrier suggests the intriguing possibility of endowing these nanoparticles with thermal responsiveness in the clinically relevant temperature range of 37–42 °C, which would allow them to be targeted in vivo to a site of disease by externally applied, focused mild hyperthermia. To our knowledge, no such thermally responsive drug-loaded nanoparticles currently exist.

The launching point of our attempt to rationally design drug-loaded, thermally targeted nanoparticles was our recent observation that the site-specific (C-terminal) covalent attachment of multiple copies of doxorubicin—a small-molecule chemotherapeutic agent—to a chimeric polypeptide (CP) resulted in the formation of near-monodisperse micelles.[2,5] This observation prompted three questions, which provided the roadmap for this study: 1) is the conjugation-triggered self-assembly of a CP as observed in the previous study restricted to a small set of compounds, or does it reflect a more general propensity of CPs to undergo self-assembly upon conjugation to small molecules? 2) If this phenomenon is indeed general, what is the mechanism that drives their self-assembly? 3) If we can uncover the rules that drive self-assembly, can we use this information to rationally design drug-loaded nanoparticles that also exhibit thermal responsiveness in the clinically relevant temperature range of 37–42 °C under physiologically relevant conditions?

To explore these questions, we covalently attached 14 different maleimide derivatives of small molecules to a CP. These model compounds were chosen with two considerations in mind: first, they span a large range of hydrophobicity, as reflected by their octanol–water distribution coefficient, Log *D*.[6] Second, they all contain a reactive maleimide moiety to enable their covalent coupling to the CP. The CP used in this study consists of two segments: a hydrophilic, biodegradable elastin-like polypeptide segment with a molecular weight of 62 kDa, and a short, 1.6 kDa cysteine-rich Cys(Gly-Gly-Cys)$_7$ segment that provides eight thiol groups for conjugation with the maleimide derivatives (Figure 1 A).

Elastin-like polypeptides (ELPs) are biopolymers consisting of repeats of the peptide sequence VPGXG (derived from tropoelastin[7]), in which the guest residue "X" can be selected from all amino acids (except Pro) to tune the biophysical properties of the polypeptide. An ELP was selected as the hydrophilic segment of the CP because it has many properties desirable for a drug carrier: ELPs can be encoded at the gene level and recombinantly overexpressed from a heterologous host, which allows precise control over the number and location of reaction sites along the backbone; they are monodisperse because they are recombinantly synthesized; they exhibit a sharp hydrophilic-to-hydrophobic phase transition in response to environmental variables (such as temperature and ionic strength), which can be tuned by modulating the biopolymer composition and molecular weight;[8,9] they are biodegradable[10] and nontoxic;[11] and they display favorable pharmacokinetics.[2,12–14] ELPs also have the important practical attributes that they can be expressed in high yield in bacterial expression systems[15] and they can be purified conveniently by exploiting their environmental sensitivity.[16,17]

The CP was overexpressed from a plasmid-borne gene in *Escherichia coli* (see the Supporting Information) and was purified by a nonchromatographic method, inverse transition cycling.[16,17] The model compounds with Log *D* values ranging from −1 to 4 were selectively conjugated to the Cys residues in the CP by a Michael addition reaction. Figure 1 B displays the structure of the model compounds with respect to their Log *D* value at pH 7.4, whereby higher values indicate greater hydrophobicity. The log *D* value was calculated with the

[*] J. R. McDaniel,[+] Dr. J. Bhattacharyya,[+] W. Hassouneh, Prof. A. Chilkoti
Department of Biomedical Engineering, Duke University
136 Hudson Hall, Box 90281, Durham, NC 27708-0281 (USA)
E-mail: chilkoti@duke.edu
K. B. Vargo, Prof. D. A. Hammer
Department of Chemical and Biomolecular Engineering
University of Pennsylvania
Philadelphia, PA 19104 (USA)
[+] These authors contributed equally.

[**] This research was supported by a grant from the National Institutes of Health (R01 EB000188) to A.C. and by the Research Triangle MRSEC of the NSF (DMR-1121107). J.R.M. acknowledges the financial support of a NIH Biotechnology Predoctoral Fellowship (T32 GM 8555).

Supporting information for this article is available on the WWW under http://dx.doi.org/10.1002/anie.201200899.

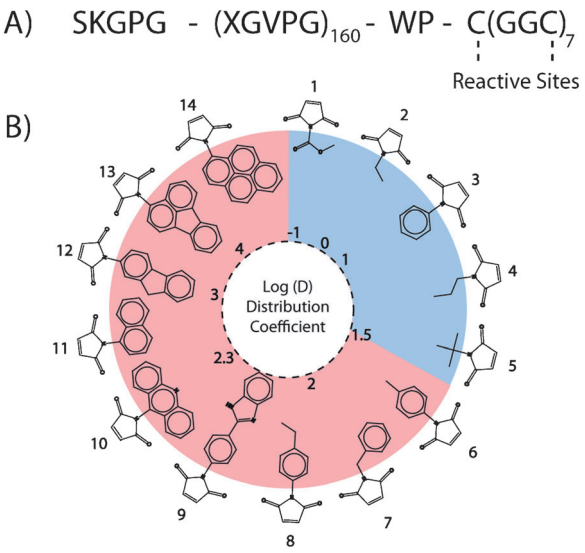

Figure 1. A) Sequence of the chimeric polypeptide. The 62 kDa ELP segment of the CP consists of 160 repeats of VPGXG, in which the guest residue X has the composition $Val_1Gly_7Ala_8$. The 1.6 kDa cysteine-rich sequence at the C terminus provides sites for the covalent conjugation of maleimide derivatives of model compounds. B) Structure of the model compounds. The circle serves as a visual map of the model compounds and their hydrophobicity as measured by the distribution coefficient at pH 7.4. The attachment of compounds with $\text{Log}\,D \leq 1.5$ (shown in blue) did not trigger self-assembly of the CP, whereas compounds with $\text{Log}\,D > 1.5$ (shown in pink) triggered self-assembly of the CP into nanoparticles.

ACD/Labs PhysChem Suite,[18] which fragments a molecule into non-overlapping structures. A summation of the hydrophobicities of the individual components and their correction factors then gives the $\log D$ value.[6,19] Following attachment, the degree of conjugation was assessed by determining the ratio of free residual cysteine residues, as quantified with the Ellman reagent, to the polypeptide concentration, as measured by the bicinchoninic acid assay (see the Supporting Information for experimental details). This ratio ranged from 3.3:1 to 6.4:1 for all of the molecules (see Table 2 in the Supporting Information).

Next, we investigated the spontaneous self-assembly of the conjugates by dynamic and static light scattering (DLS, SLS), temperature-programmed turbidimetry, and fluorescence spectroscopy (see Figure 2 in the Supporting Information for fluorescence data). The attachment of 3–6 copies of compounds with a $\log D$ value less than 1.5 (shown in blue in Figure 1 B) did not trigger self-assembly of the CP, whereas compounds with a $\log D$ value above 1.5 (shown in pink) imparted sufficient amphiphilicity to the CP to trigger self-assembly of the CPs into nanoparticles, in which the conjugated molecules presumably form the hydrophobic core. The conjugates that did not trigger self-assembly had an average hydrodynamic radius (R_h) of (5.9 ± 0.7) nm, which is similar to the R_h value of the unmodified, control CP. In contrast, the conjugates that formed nanoparticles had an R_h value ranging from 30 to 58 nm, with an average standard deviation of approximately 15% within each population (Figure 2 B). There was no correlation between the hydrodynamic size of the nanoparticles and the number of small molecules conjugated per CP molecule ($R^2 = 0.0009$).

Each nanoparticle-forming conjugate was next analyzed by SLS to determine the number of CP molecules per nanoparticle and the shape factor ($\rho = R_g/R_h$), which describes the distribution of mass within the nanoparticle. The shape factors ranged from 0.69 to 1; this broad range indicates that there are probably significant differences in the morphology of some of these nanoparticles. It is not possible to precisely determine the morphology of nanoparticles by light scattering, as the shape factor is subject to deviations arising from polydispersity and shape diversity within the ensemble of nanoparticles. Shape factors of 0.775 are indicative of spherical micelles, which are probably the form of nanoparticles with $\rho = 0.69$–0.8, whereas nanoparticles with shape factors of about 1.0 could instead be vesicles, as spherical shells have a ρ value of 1.0, or polydisperse rods with relatively low aspect ratios.[20] The apparent coordination number (Z) also varied significantly between about 10 and 60 for the different conjugates. The apparent coordination numbers were not corrected for the critical aggregation concentration (CAC) of the nanoparticles; therefore, the numbers shown in Figure 4 are probably the minimum coordination numbers for each nanoparticle. There was a trend toward larger apparent coordination numbers as the hydrophobicity of the conjugated molecules increased (Figure 4).

To directly visualize the morphology and shape diversity of the nanoparticles, we imaged selected conjugates by cryogenic transmission electron microscopy (cryo-TEM). We imaged the samples at 80 keV to increase the contrast between the environment and the nanoparticle core, which exhibited a relatively high aqueous content. The conjugates formed from maleimide derivatives with $\text{Log}\,D > 1.5$ formed nanoparticle cores distributed throughout the ice at regular intervals (Figure 3 B–F), whereas a film devoid of any structures was observed for the one hydrophilic conjugate displayed (Figure 3 A). In agreement with the light-scattering data, the selected conjugates primarily consisted of spherical nanoparticles, although in a few of the samples there were subpopulations of wormlike micelles and stiff rods present, which may explain the variability in the shape factor measured by light scattering (see Figure 1 in the Supporting Information).

These data clearly demonstrate that the attachment-triggered self-assembly of a CP is possible with a diverse range of hydrophobic small molecules. These results also reveal a simple predictive rule that governs the self-assembly of CPs and is based on a threshold hydrophobicity of the conjugated small molecule. Although the threshold of $\text{Log}\,D > 1.5$ predicts whether self-assembly will occur, the $\text{Log}\,D$ value of the conjugated molecule does not predict the size or shape of the nanoparticle that is formed, as we observed significant differences in both parameters on the basis of the light-scattering results. These differences are most likely related to structural differences between the molecules.

We also found that the phase-transition behavior of the CP was altered following conjugation of the model compounds (Figure 2 A). CPs, in a similar way to the ELPs from

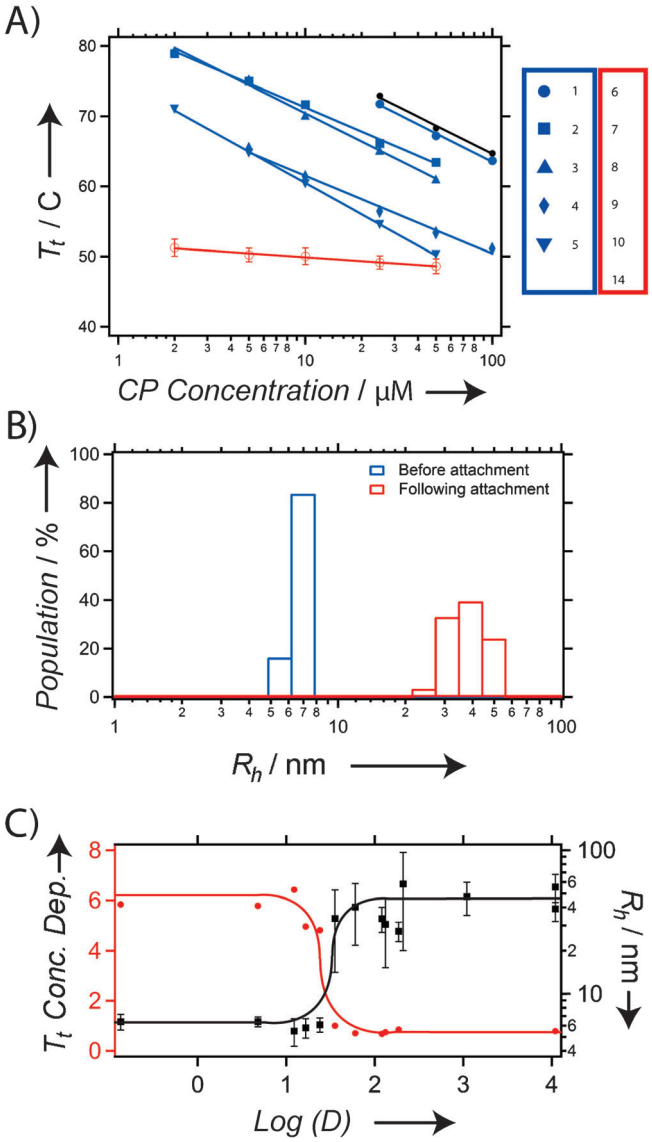

Figure 2. Physical properties of the CP nanoparticles. A) Thermal characterization of the CP in terms of the transition temperature (T_t) as a function of the CP concentration of CPs conjugated to hydrophilic compounds (blue: unimer; compounds **1**–**5**) and hydrophobic compounds (red: nanoparticle; compounds **6**–**10**, **14**) as compared with an unconjugated control (black: unimer). The thermal behavior of all six CP–small-molecule conjugates that formed nanoparticles was identical and is hence plotted as the mean T_t value of the CP–small-molecule conjugates; the error bars are the standard deviation. The lines are linear fits to the data. B) DLS results for the CP conjugate of compound **8** (Log $D = 2.1$). The graph shows the increase in R_h from approximately 6 nm, which corresponds to the presence of unimers prior to conjugation, to approximately 33 nm after conjugation and the formation of nanoparticles. C) Relationship between T_t (left-hand y axis, data in red) and R_h (right-hand y axis, data in black) as a function of Log D for all 14 conjugates. As the Log D value increases to greater than 1.5, the particle R_h value increases from 6 nm (unimer size) to 30–55 nm (nanoparticles), depending on the conjugate. The concentration dependence of the T_t value (slope from (A)) decreases from an average value of −5.5 to −1.0 °C/Log(concentration). The curves in (C) are solely a guide to the eye.

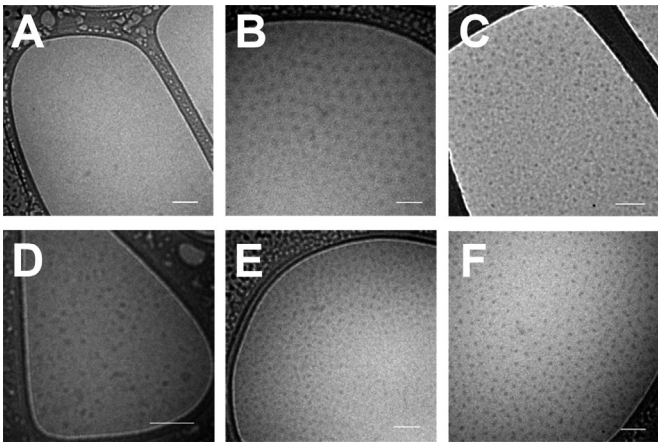

Figure 3. Cryo-TEM images of CP conjugates in phosphate-buffered saline. A) The CP conjugate with *N*-methoxycarbonylmaleimide (**1**) did not form nanoparticles and is displayed as a negative control. The CP conjugates with B) *n*-benzylmaleimide (**7**), C) *n*-[4-(2-benzimidazolyl)-phenyl]maleimide (**9**), D) 2-maleimidofluorene (**12**), E) *n*-(1-pyrenyl)-maleimide (**14**), and F) paclitaxel spontaneously formed nanoparticles. Scale bars: 100 nm.

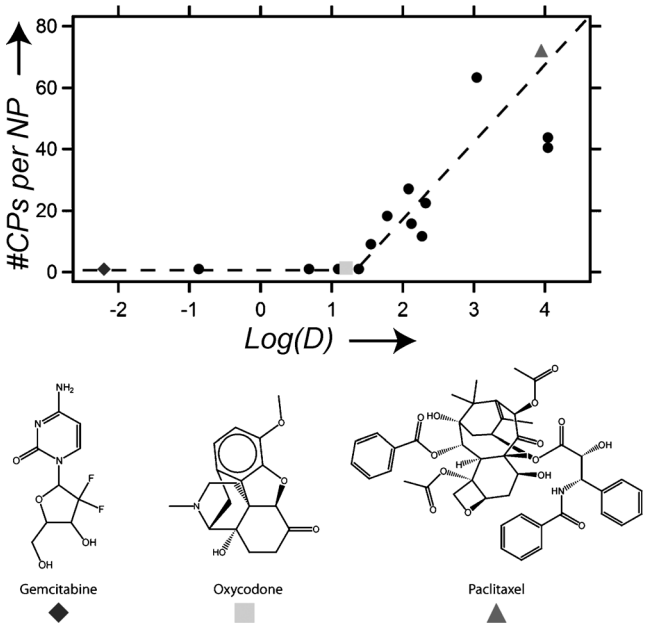

Figure 4. Apparent coordination number (number of CP molecules per nanoparticle, #CPs/NP) versus the Log D value of the small molecules conjugated to each CP molecule. Above the threshold of Log $D \approx 1.5$, the number of CP molecules per nanoparticle increases with the hydrophobicity of the conjugated small molecule (Log D). The diamond, square, and triangle markers indicate gemcitabine, oxycodone, and paclitaxel, respectively. The dashed line is solely a guide to the eye.

which they are derived, display a characteristic transition temperature (T_t), below which they are soluble in aqueous solutions, and above which they form polydisperse micron-sized aggregates. This T_t value is typically modulated by varying the hydrophobicity of the guest residue (X), whereby hydrophobic guest residues depress the T_t value, and hydro-

philic residues elevate the T_t value.[9] In a similar manner, as the hydrophobicity of the conjugated molecules increased to the assembly threshold as defined by Log $D = 1.5$, the T_t value shifted downward, although the dependence upon concentration (the slope) remained uniform (Figure 2A). When this threshold was reached, however, the T_t value immediately decreased to a temperature that was nearly independent of concentration, although we note that this transition occurs from a nanoparticle to micron-sized aggregates in contrast to unmodified CPs, which undergo a transition from soluble unimers to micron-sized aggregates. Notably, all conjugates that form nanoparticles displayed the same thermal behavior, which is described by the same quantitative relationship between T_t and the CP unimer concentration. The fact that all self-assembled CP nanoparticles display the same functional relationship between their T_t value and their solution concentration (on a unimer basis) strongly suggests that their phase behavior is controlled by the high and invariant local ELP concentration within the nanoparticles and not by the total concentration of the CP in solution.

This finding is significant because the near independence of T_t from the CP concentration enables the nanoparticles to maintain a very stable T_t value (within 2 °C) over a 100-fold decrease in concentration that would arise from physiological effects, such as clearance from circulation. In contrast, unmodified CP and the CP conjugates that exist as unimers show a T_t shift of over 20 °C within the same concentration range (Figure 2A). The ability of these thermoresponsive nanoparticles to maintain a constant thermal response over a range of concentrations eliminates the need to compensate for the effect of dilution and clearance that would occur upon their injection into systemic circulation and is hence likely to be an extraordinarily useful feature in future attempts to thermally target these CP nanoparticles to specific tissues in vivo by the application of external focused hyperthermia to disease sites.

These experiments with model compounds provide a simple physical model for self-assembly, in that molecules with Log $D > 1.5$ will drive the self-assembly of the conjugate into nanoparticles. To further investigate the predictive validity of this model, we selected three small-molecule therapeutic agents for conjugation to the CP through heterobifunctional linkers, whereby one end of the linker was attached to the CP and the other end to a reactive moiety on the drug (see the Supporting Information for methods). We chose three drugs that spanned a range of Log D values at pH 7.4, as estimated by the ACD/Labs PhysChem Suite:[18] gemcitabine (−2.2), oxycodone (1.2), and paclitaxel (4.0). The conjugation of gemcitabine and oxycodone did not trigger self-assembly of the CP, whereas the conjunction of paclitaxel led to the spontaneous formation of nanoparticles that were similar in size to the nanoparticles that self-assembled upon the attachment of hydrophobic small molecules to the CP (Table 1 and Figure 4). The conjugation of paclitaxel to the hydrophilic CP also significantly increased the solubility of paclitaxel in excess of 2 mM paclitaxel equivalents in phosphate-buffered saline. The solubility of paclitaxel was ultimately limited by the viscosity of the CP solution. Cryo-TEM of the CP–paclitaxel nanoparticles displayed close-packed spherical nanoparticles with an electron-dense core, whose size (measured in terms of the core-to-core distance) was smaller than the R_h value determined by dynamic light scattering ($R_{TEM} = 22 \pm 4$ nm, $n = 50$; Figure 3F). This discrepancy is probably due to the fact that the soft CP-nanoparticle corona can become significantly compressed under the conditions necessary to visualize the particles by cryo-TEM (the high shear stress induced by blotting and the high polymer concentration) in comparison with the very dilute conditions necessary for light-scattering measurements. The CP–paclitaxel nanoparticles were also highly stable (CAC ≤ 10 μM; see Figure 3 in the Supporting Information). These results are consistent with the model: gemcitabine and oxycodone, as predicted by the model, were too hydrophilic to drive the assembly of nanoparticles at pH 7.4, whereas paclitaxel, with a Log D value of 4.0, is above the threshold of hydrophobicity needed to trigger self-assembly.

Table 1: CP nanoparticles assembled through drug conjugation.

Drug	Log D[a]	R_h [nm]	Drug/CP	#CPs/NP
gemcitabine	−2.2	5.7	5:1	0.9
oxycodone	1.2	9.7	4:1	1.3
paclitaxel	4.0	53.3	2:1	72.0

[a] The Log D value was estimated by using the ACD/Labs PhysChem Suite.

Having shown that we can rationally design and synthesize a drug-loaded CP nanoparticle, we next turned our attention to the construction of a thermally responsive CP nanoparticle that would be useful for in vivo targeting. We synthesized a CP, termed CP_2, with a V_1A_9 guest-residue composition, which is slightly more hydrophobic than the $V_1G_7A_8$ sequence used throughout the rest of this study (CP_1), to decrease its T_t value to the desired range of 37–42 °C, on the basis of a large body of structure–property relationships that we have assembled for ELPs in the past decade. CP_2 exhibited a T_t value between 38 and 42 °C in 90 % fetal bovine serum, a medium that closely mimics in vivo conditions. The T_t value was invariant for three different CP_2 nanoparticle conjugates with small molecules with Log D values in the range from 1.5 (compound **6**) to 4.0 (compound **14**; Figure 5). These nanoparticles were stable in serum, as the T_t value remained characteristically near-independent of the concentration of the CP in solution.

The attachment of drugs to polymers has been used previously for the development of self-assembling therapeutic formulations: adriamycin was covalently conjugated to the aspartate groups in PEG_{4300}-*b*-polyaspartate (NK911), which then assembled into 50 nm micelles;[21] the biologically active metabolite of irinotecan, SN-38, was attached to the glutamate chain in PEG_{5000}-*b*-polyglutamate (NK012) to form micelles;[22] and the polyaspartate chain of PEG_{12000}-*b*-polyaspartate was modified with 4-phenyl-1-butanol, which induced assembly and facilitated the noncovalent incorporation of paclitaxel into (NK105).[23] However, our approach departs significantly both in its conceptual novelty and scope from these previous studies, in which a general route to the conjugation-triggered self-assembly of the polymer by a range of molecules was not shown; nor did these and related studies

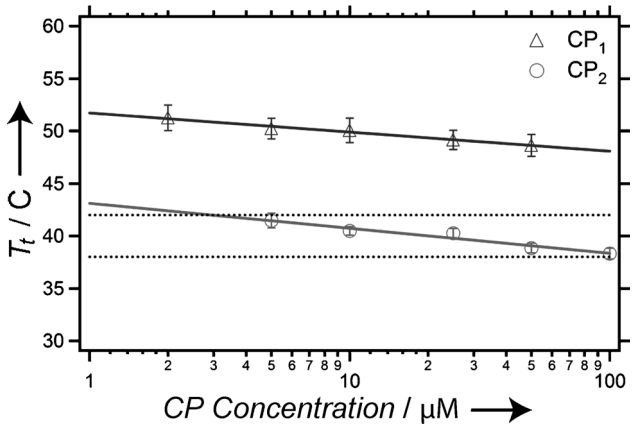

Figure 5. Design of thermally sensitive CP nanoparticles. The graph shows the transition temperature (T_t) as a function of the CP_1 and CP_2 concentration. The data shown for CP_1 are average values for conjugates with **6**–**10** and **14**, whereas the data for CP_2 are average values for conjugates with **6**, **7**, and **14**. The dotted lines show the targeted temperature range for hyperthermia (38–42 °C). The error bars are the standard deviation. The unbroken lines are linear fits to the data.

provide a model that enabled the prediction of the propensity—or lack thereof—of a molecule to trigger the self-assembly of the polymer.[21,24–26] Furthermore, none of these systems exhibited the thermal responsiveness observed for the CPs in this study over a range of concentrations relevant for drug delivery. This feature can be exploited for the in vivo thermal targeting of CP–drug nanoparticles.

In conclusion, this study is the first demonstration of a roadmap for the rational design of highly soluble, thermally responsive drug-loaded nanoparticles whose properties can be tailored at the molecular level. We have shown that the attachment of small molecules above a critical threshold of hydrophobicity triggers self-assembly of the CP into soluble nanoparticles ranging from 60 to approximately 100 nm in diameter. These nanoparticles are soluble at concentrations greater than 100 μM in the CP and approximately 300—600 μM in the small molecule, and are stable upon dilution to low-micromolar concentrations of the CP: a concentration regime that is of great utility for drug delivery. These results demonstrate that conjugation-triggered self-assembly can package a hydrophobic drug into soluble nanoparticles and provide a simple predictive model for nanoparticle formation that enables the propensity of drugs to be sequestered into the nanoparticle core to be determined solely on the basis of their Log *D* value. Finally, we have demonstrated that we can rationally tune the nanoparticle-to-aggregate T_t value to occur between 38 and 42 °C to provide a nanoparticle drug-delivery system that can be targeted to diseased tissue by externally applied, focused mild hyperthermia.

Received: February 1, 2012
Revised: November 27, 2012
Published online: December 20, 2012

Keywords: biopolymers · distribution coefficient · elastin-like polypeptides · self-assembly · thermoresponsive nanoparticles

[1] R. Duncan, *Nat. Rev. Cancer* **2006**, *6*, 688–701.
[2] J. A. MacKay, M. N. Chen, J. R. McDaniel, W. G. Liu, A. J. Simnick, A. Chilkoti, *Nat. Mater.* **2009**, *8*, 993–999.
[3] H. Maeda, L. W. Seymour, Y. Miyamoto, *Bioconjugate Chem.* **1992**, *3*, 351–362.
[4] F. M. Veronese, C. Monfardini, *Bioconjugate Chem.* **1998**, *9*, 418–450.
[5] J. R. McDaniel, S. R. Macewan, M. Dewhirst, A. Chilkoti, *J. Controlled Release* **2012**, *159*, 362–7.
[6] D. J. Livingstone, *Curr. Top. Med. Chem.* **2003**, *3*, 1171–1192.
[7] D. W. Urry, T. L. Trapane, K. U. Prasad, *Biopolymers* **1985**, *24*, 2345–2356.
[8] D. E. Meyer, A. Chilkoti, *Biomacromolecules* **2004**, *5*, 846–851.
[9] D. W. Urry, *J. Phys. Chem. B* **1997**, *101*, 11007–11028.
[10] M. F. Shamji, H. Betre, V. B. Kraus, J. Chen, A. Chilkoti, R. Pichika, K. Masuda, L. A. Setton, *Arthritis Rheum.* **2007**, *56*, 3650–61.
[11] D. W. Urry, T. M. Parker, M. C. Reid, D. C. Gowda, *J. Bioact. Compat. Polym.* **1991**, *6*, 263–282.
[12] H. Betre, W. Liu, M. R. Zalutsky, A. Chilkoti, V. B. Kraus, L. A. Setton, *J. Controlled Release* **2006**, *115*, 175–182.
[13] W. Liu, M. R. Dreher, D. C. Chow, M. R. Zalutsky, A. Chilkoti, *J. Controlled Release* **2006**, *114*, 184–192.
[14] W. E. Liu, M. R. Dreher, D. Y. Furgeson, K. V. Peixoto, H. Yuan, M. R. Zalutsky, A. Chilkoti, *J. Controlled Release* **2006**, *116*, 170–178.
[15] A. Chilkoti, D. C. Chow, M. R. Dreher, K. Trabbic-Carlson, *Biotechnol. Prog.* **2006**, *22*, 638–646.
[16] D. E. Meyer, A. Chilkoti, *Nat. Biotechnol.* **1999**, *17*, 1112–5.
[17] K. Trabbic-Carlson, L. Liu, B. Kim, A. Chilkoti, *Protein Sci.* **2004**, *13*, 3274–84.
[18] Advanced Chemical Development, Inc., 133 Richmond Street West, Suite 605, Toronto, Canada M5H 2l3.
[19] A. A. Petrauskas, E. A. Kolovanov, *Perspect. Drug Discovery Des.* **2000**, *19*, 99–116.
[20] I. Manners, J. Massey, K. N. Power, M. A. Winnik, *J. Am. Chem. Soc.* **1998**, *120*, 9533–9540.
[21] M. Yokoyama, M. Miyauchi, N. Yamada, T. Okano, Y. Sakurai, K. Kataoka, S. Inoue, *Cancer Res.* **1990**, *50*, 1693–1700.
[22] F. Koizumi, M. Kitagawa, T. Negishi, T. Onda, S. Matsumoto, T. Hamaguchi, Y. Matsumura, *Cancer Res.* **2006**, *66*, 10048–10056.
[23] T. Hamaguchi, Y. Matsumura, M. Suzuki, K. Shimizu, R. Goda, I. Nakamura, I. Nakatomi, M. Yokoyama, K. Kataoka, T. Kakizoe, *Br. J. Cancer* **2005**, *92*, 1240–1246.
[24] K. Kataoka, Y. Bae, S. Fukushima, A. Harada, *Angew. Chem.* **2003**, *115*, 4788–4791; *Angew. Chem. Int. Ed.* **2003**, *42*, 4640–4643.
[25] K. Kataoka, N. Nishiyama, S. Okazaki, H. Cabral, M. Miyamoto, Y. Kato, Y. Sugiyama, K. Nishio, Y. Matsumura, *Cancer Res.* **2003**, *63*, 8977–8983.
[26] G. Kwon, M. Naito, M. Yokoyama, T. Okano, Y. Sakurai, K. Kataoka, *Langmuir* **1993**, *9*, 945–949.

